Int. J. Multiphase Flow Vol. 16, No. 6, pp. 959–974, 1990
Printed in Great Britain

0301-9322/90 $3.00 + 0.00
Pergamon Press/Elsevier

ANALYSIS OF THE DRYOUT INCIDENT IN THE OSKARSHAMN 2 BOILING WATER REACTOR

K. M. BECKER,[1] J. ENGSTRÖM,[2] O. NYLUND,[2] B. SCHÖLIN[2] and B. SÖDERQUIST[1]

[1]Royal Institute of Technology, 100 44 Stockholm, Sweden

[2]ABB Atom AB, 721 63 Västerås, Sweden

(*Received* 27 *September* 1989; *in revised form* 5 *May* 1990)

Abstract—Early in 1988 dryout of fuel rods occurred in the Oskarshamn 2 boiling water reactor. During refuelling it was observed that one corner rod was damaged in each of four fuel assemblies. These were of the SVEA design, SVEA being the trade name of the ABB Atom water cross fuel. The damaged zone covered about 180° of the rod periphery facing the corner sub-channel, over a stretch of about 30 cm with the upper end just below the last downstream spacer.

The dominating cause of the dryout was re-use of fuel channels for ordinary 64-rod fuel, which were located in neighbouring positions to the SVEA fuel. The re-used channels showed excessive bowing because of irradiation. This bow increased the water gap between the fuel assemblies, thus increasing the neutron moderation and the local power around one corner of the SVEA fuel. This and some other factors caused the local peaking factor for the corner rod to increase from ~1.04 to ~1.38.

The flow and power conditions in the damaged fuel assemblies were calculated by means of the POLCA, PHOENIX, CASMO and CONDOR computer programs. The results of these calculations were used as a base for dryout predictions, which were carried out employing eight correlations, which are available in the open literature. The Barnett, the Becker and the Bezrukow correlations predicted the dryout power within 1%. Also the Condie & Bengston, the EPRI and the XN-1 correlations yielded very good results with accuracies of, respectively, −5.1, −2.3 and 7.3%. The Becker, the XN-1, the Bezrukow and the Condie & Bengston correlations predicted dryout to occur inside of the observed dryout zone of 30 cm length.

It is concluded that the dryout in the Oskarshamn 2 nuclear power plant was not caused by any faults in the design or manufacture of the SVEA fuel, and that the re-use of fuel channels should not be permitted.

Key Words: critical heat flux, dryout, burnout, post-dryout

1. INTRODUCTION

During the refuelling outage in August 1988 of the Oskarshamn 2 boiling water reactor, four failed fuel assemblies were identified through sipping. In the preceding cycle, offgas and primary system water activity had shown fuel leakage to develop stepwise in the period from January to February. From inspections it was subsequently concluded that dryout had caused the fuel rod failure through heavy cladding oxidation of one single rod at the control rod corner in each of the four assemblies. The dryout region was located immediately below the topmost spacer grid and water intrusion had given rise to secondary cladding failures near the bottom end. Dryout had occurred over a stretch of about 30 cm. The damaged zone did not cover the total periphery of the rod, but rather about 180° facing the corner sub-channel of the bundle.

All types of events that could have caused dryout, such as full power normal operation, nuclear heating at low system pressure, a power ascension at the end of December, possible transients and operator errors were investigated. It was concluded that dryout occurred at full, steady-state power since reanalysis of the operation explains the failures, and other possibilities could be ruled out.

This dryout incident offers, indeed, an interesting possibility to carry out assessments of computer codes and dryout correlations as well as post-dryout heat transfer correlations. In the present report predictions of the Oskarshamn 2 in-pile dryout conditions are presented, employing a number of the mostly used rod bundle dryout correlations, which are available in the open literature.

2. TYPE OF FUEL AND CAUSE OF FUEL ROD OVERPOWER

The damaged fuel was of the type SVEA-64, which is a trade name for the ABB Atom water cross fuel with 64 rods. The water cross, which divides the assembly into four channels, each

containing a 4 × 4 rod bundle, as shown in figure 1, improves the neutron moderation and thus increases reactivity and decreases local power and burnup peaking factors. It also improves the mechanical structure of the channel, so that lattice improvements can be made by decreasing the control rod gaps.

The Oskarshamn 2 reactor was in a phase of transition from the previous standard 8 × 8 fuel to the SVEA type. At the incident there was about 40% SVEA fuel. A much greater portion than 40% of the power was generated in this fuel, because it was recently loaded and had initially considerably increased reactivity. The minimum dryout margin evaluated in the core supervision was around 1.30. Two main causes for the loss of this margin have been identified:

I. Channel bow of neighbouring 8 × 8 assemblies

The failed SVEA assemblies were all located in supercells with two 8 × 8 assemblies, as shown in figure 2. The latter fuel assemblies had re-used channels of high exposure. Large channel bows have been measured on the adjacent 8 × 8 assemblies in the central supercell. Mid-channel values were in the range 7–8 mm. Bow measurements are not available for the other supercells, but gamma scans of a number of fuel rods in one of the SVEA assemblies indicated the existence of large channel bow also in this case. Channel bow of the 8 × 8 assemblies implies heavily tilted power distributions in the SVEA assemblies, leading to increased power peaking factors and reduced dryout margins. Of course the 8 × 8 assemblies were affected in the same way. Dryout did not occur in these assemblies due to high burnup and lower initial reactivity and thus much lower

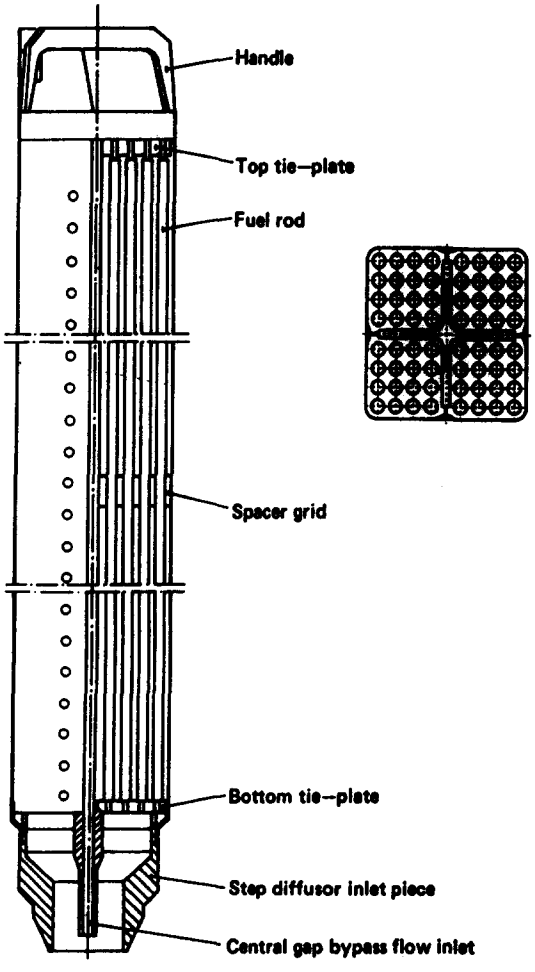

Figure 1. SVEA fuel assembly.

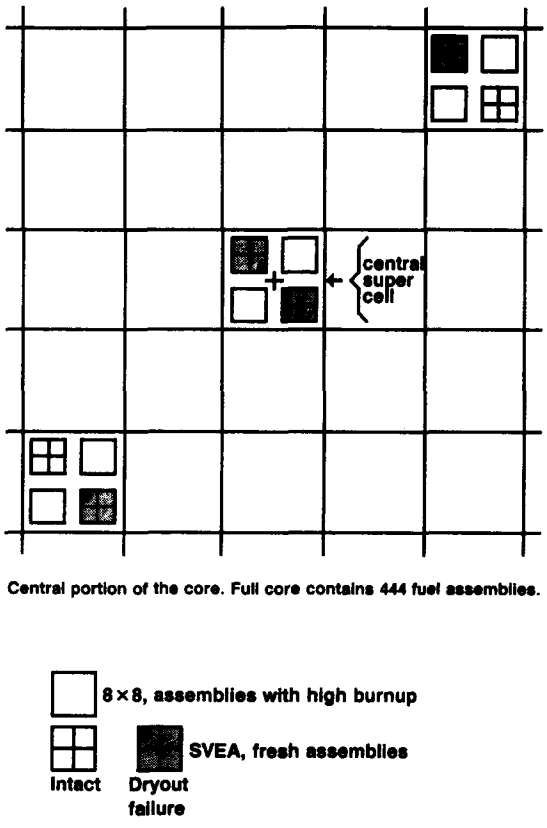

Figure 2. Location of failed assemblies in the Oskarshamn 2 core.

assembly power. Accelerated axial growth at high exposure has been identified as the cause of the large channel bow.

II. Core supervision in a core with mixed water gaps

SVEA assemblies for the asymmetric lattice of the Oskarshamn 2 core are designed to improve the lattice geometry by making the lattice more symmetric. This means that the water gaps around the fuel assemblies are made more equal by adjusting the position of the assemblies. This has advantages with regard to reactivity and enrichment distributions. It also reduces the fast neutron flux difference between opposite channel walls, which provides the driving force for channel bow. Introducing relocated fuel assemblies implies that special care has to be taken in the core supervision. Power peaking factors should be modelled correctly for the mixed gap situation throughout the transition period. However, this was not done in the present case.

These two effects, as illustrated in figure 3, resulted in much enlarged water gaps and a corresponding local improvement of the neutron moderation and power increase in the fuel rods facing these gaps. In particular, the power in the corner rods of the SVEA bundles became very high. Figure 4 shows the rod power distribution used in the core supervision and as recalculated with the enlarged gaps according to figure 3(C). The 8 × 8 channel bow was chosen to be 4.5 mm, which is about 60% of the measured mid-channel bow. The justification for the use of this value for the present dryout assessments is discussed later. Based on manufacturing data the SVEA assemblies has a mean bow of ~0.5 mm away from the control rod. The recalculated power distribution is seen to be strongly tilted and an average rod peaking factor of 1.38, normalized to 63 active rods, is found for the corner rod facing the centre of the supercell. This high local power, which was unknown to the reactor operating personnel, caused the dryout to occur on the corner rod.

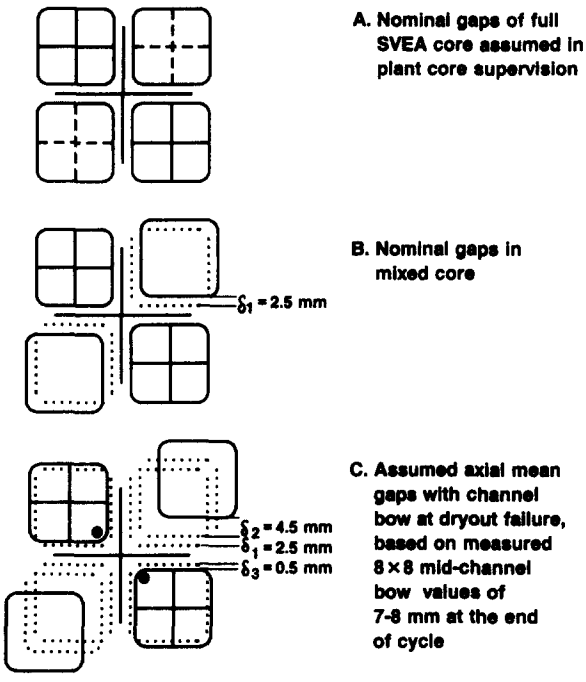

Figure 3. Water gap changes in the Oskarshamn 2 core cell.

It should also be noted that all the SVEA assemblies in the supercells in which the failures occurred were operating in their first cycle. This means that they were in a phase of increasing power as their content of burnable absorber was being depleted. The high local power also caused a high depletion rate of the burnable absorber in this region. Dryout therefore occurred earlier in the cycle than the predicted minimum dryout margin according to the core supervision calculations.

3. CONDITIONS IN THE FUEL ASSEMBLIES AT DRYOUT

Visual observation of the failed fuel assemblies after removal from the reactor showed, for one corner rod in each assembly, a distinct dryout area covering an axial stretch starting at about $z = 310$ cm and ending at $z = 339$ cm from the inlet. The end of the dryout zone was just below the upper spacer. The length of the heated section was 371.2 cm. The excessive heating covered

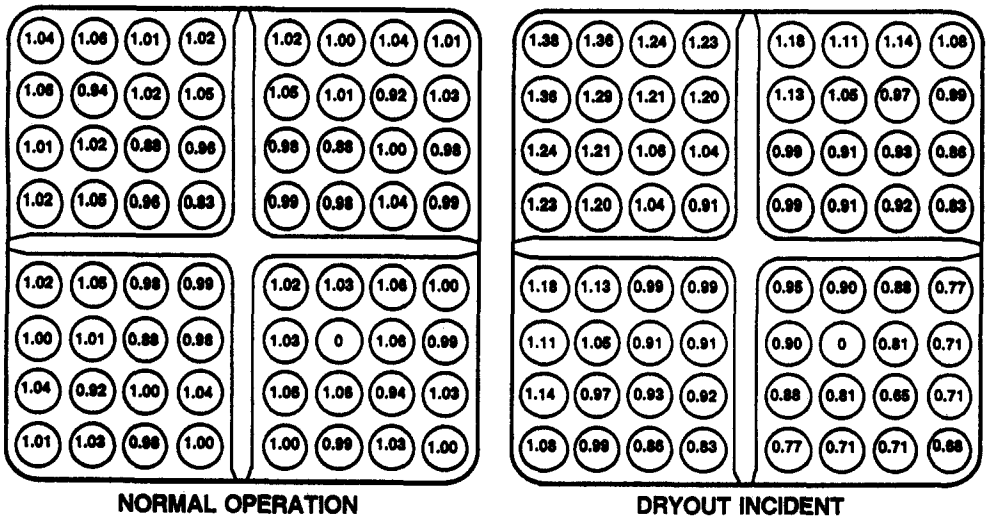

Figure 4. Local power distribution.

approx. 180° of circumference of the rod; 90° facing the corner sub-channel and about 45° facing each of the two neighbouring sub-channels as shown in figure 5.

In the dryout area the Zircaloy cladding was severely damaged due to oxidation. Figure 6 shows a portion of one of the damaged rods photographed during hot cell examinations. Metallurgical investigations by Johnson (1989) indicated that the temperature of the remaining metal in the dryout zone had reached $\sim 1000°C$.

The reactor instrumentation readings, which were continuously processed by the plant computer, provided sufficient information in order to calculate the flow conditions and the power distribution in the fuel element when dryout occurred. The calculations were carried out by means of the POLCA (Olsson 1983; Lindahl 1983), PHOENIX (Olsson 1983; Stamm'ler & Veenhuizen 1987), CASMO (Edenius & Ahlin 1988) and CONDOR (Olsson 1983; Lindahl 1983) computer programs.

The reactor pressure and the coolant inlet temperature were:

$$P = 70.5 \text{ bar and } T_i = 275°C.$$

The POLCA calculations yielded the following results for SVEA assemblies in the supercells according to figure 2:

central supercell,

bundle power $Q = 5.80$ MW

mass flow rate $\dot{m} = 9.90$ kg/s;

and

outer supercells,

bundle power $Q = 6.20$ MW

mass flow rate $\dot{m} = 9.50$ kg/s.

The central supercell was chosen for the present assessment because the channel bow situation is best known in this case.

The rod power distribution of an SVEA assembly in the central supercell, with mean channel deflections according to figure 3(C), has already been shown in figure 4. It was calculated with the PHOENIX program. The assumption of an axial mean deflection of about 60% of the measured midchannel values for 8 × 8 channels accounts for the axial variation of the channel deflection, and further for the possibility that the maximum deflection could have been somewhat smaller when the dryout occurred. The axial power distribution, obtained by POLCA, is shown in figure 7.

The large difference between the powers in the four quadrants of the fuel has a significant influence on the mass flow rate through the quadrants. The CONDOR program was used to calculate the flows, and for the quadrant where dryout occurred the following result was obtained:

mass flow rate $\dot{m} = 2.13$ kg/s.

Reverting to figure 4, the power and the local peaking factor for this quadrant are:

fuel bundle power $Q = 1.766$ MW

and

internal peaking factor $F_i = 1.152$

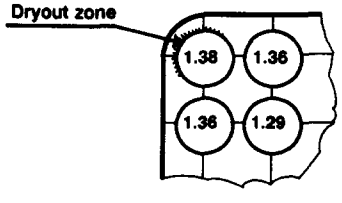

Figure 5. Circumferential position of the dryout zone.

Figure 6. Hot cell pictures of the lower end of the dryout zone.

Thus, the dryout predictions carried out in the following paragraphs, were based on the following parameters:

No. of rods	$N = 16$
Inlet temperature	$T_i = 275°C$
Mass flow rate	$\dot{m} = 70.5$ bar
Internal peaking factor	$F_i = 1.152$
Fuel rod diameter	$d = 12.25\ 10^{-3}$ m
Heated length	$L = 3.712$ m
Channel cross-section	$F = 24.28\ 10^{-4}$ m^2

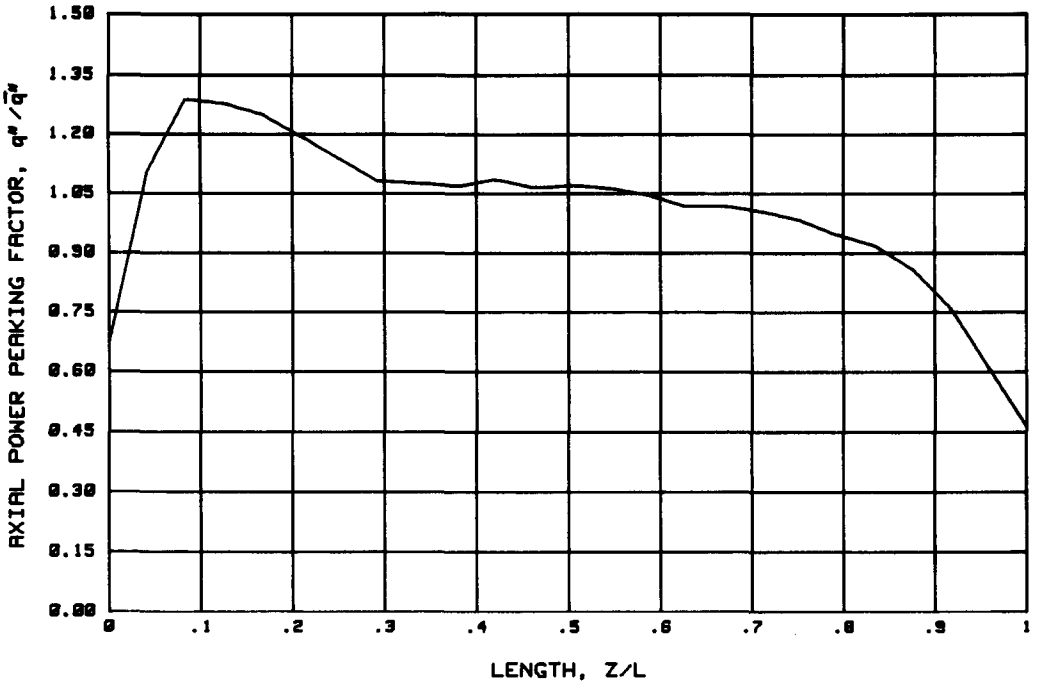

Figure 7. Axial power distribution for the SVEA fuel assembly at the Oskarshamn 2 dryout accident.

Equivalent diameter $D_e = 11.14\ 10^{-3}$
Heated equivalent diameter $D_H = 15.77\ 10^{-3}$ m.

4. DRYOUT CORRELATIONS

The following dryout correlations were employed in the present study:

1. Barnett (1966).
2. Becker (1967).
3. Bezrukow *et al.* (1976).
4. Biasi *et al.* (1967).
5. Condie & Bengston (1978).
6. CISE (Gaspari *et al.* 1974).
7. EPRI (Reddy & Fighetti 1983).
8. XN-1 (Steves *et al.* 1972).

The reason for including the Biasi correlation, which actually is a round tube correlation, was the fact that this correlation has been included in the RELAP (Ransom *et al.* 1985) and TRAC (Liles & Mahassi 1986) computer programs.

5. METHOD OF PREDICTIONS

For dryout predictions of systems with variable axial heat flux the following methods are available:

1. Total power hypothesis (Lee & Obertelli 1963).
2. Boiling length hypothesis (Bertoletti *et al.* 1965).
3. Tong's F-factor (Tong 1965).
4. Local hypothesis (Becker *et al.* 1969; Little 1970).

In the present study the local as well as the total power hypothesis were employed.

The total power hypothesis assumes the axial power distribution to be uniform. The dryout power is then easily calculated, but no information about the axial dryout position is obtained.

The employment of the local power hypothesis, however, yields the dryout power as well as the axial dryout position. Figure 8 shows the principle of the local hypothesis in a plot of the heat flux, q'', vs the steam quality, x. For the bundle operating conditions the heat flux is plotted vs the steam quality along the bundle. The dashed line refers to the average heat flux and the solid line refers to the highest loaded rod. The steam quality is the average value over the cross-section, neglecting steam quality and mass velocity variations between the sub-channels of the fuel element.

For a given pressure, inlet water temperature, mass velocity and geometry any dryout correlation can be reproduced in a heat flux vs steam quality plot, as shown in figure 8. The heat balance equation for an arbitrary axial position can be written as

$$x = \frac{Q(z)}{GFh_{LG}} - \frac{\Delta h_s}{h_{LG}} = \frac{Q \int_0^{\frac{z}{L}} F_A\left(\frac{z}{L}\right) d\left(\frac{z}{L}\right)}{GFh_{LG}} - \frac{\Delta h_s}{h_{LG}}. \quad [1]$$

The equation reveals the existence of a linear relationship between the steam quality, x, and the fuel element power, Q, for all axial positions, z. A family of straight lines, representing an arbitrarily chosen number of axial positions can be drawn. The crossing points between the straight lines and the correlation yields a family of dryout heat fluxes and a family of dryout margins:

$$\eta_{DOz} = \frac{q''_{DOz}}{q''_z}. \quad [2]$$

The axial position, z which gives the minimum values of η_{DO}, is the axial dryout position z_{DO}, and the corresponding intersection between the heat balance line and the correlation determines the dryout heat flux, q''_{DO}. The fuel element dryout power is then readily obtained by means of figure 7.

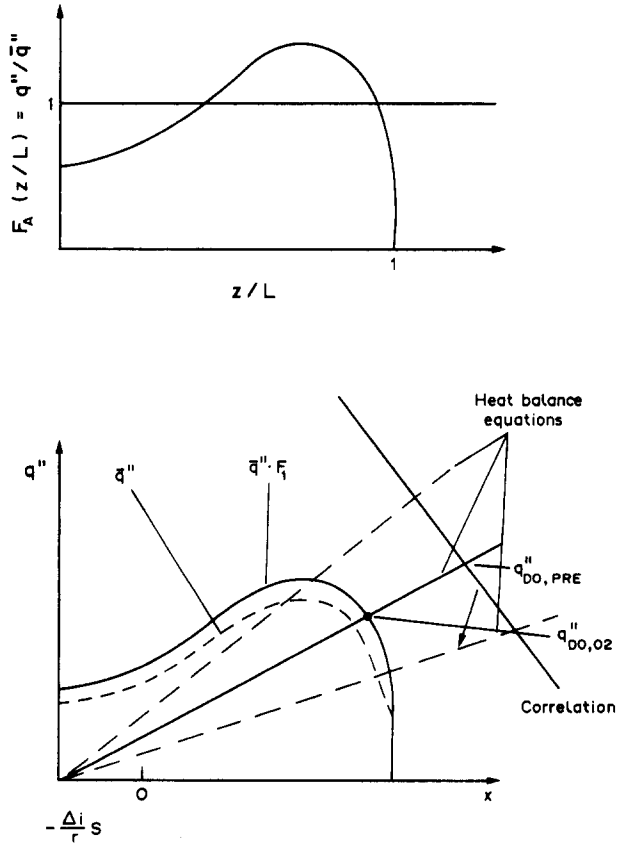

Figure 8. Principle of the local hypothesis.

At the Royal Institute of Technology a computer program is available, which employs the local hypothesis as well as the total power hypothesis and where any of the previously mentioned dryout correlations can be used.

6. RESULTS AND DISCUSSIONS

In the present study dryout predictions were carried out for the total power hypothesis as well as for the local hypothesis.

6.1. Total power hypothesis

The results for the total power hypothesis are shown in table 1. The errors E were defined as $(Q_{DO,PRE} - Q_{DO,02})/Q_{DO,02}$. Remembering that the dryout power in the Oskarshamn 2 failed SVEA sub-bundle was 1.77 MW, the results reveal that the Barnett, Becker, Bezrukow, CISE 4, EPRI and XN-1 correlations are in satisfactory agreement with the dryout incident. It should be recognized that since the dryout in Oskarshamn 2 covered a ~ 0.3 m long stretch the actual dryout power was somewhat lower than 1.77 MW. Further, the effects of the spacers are not included in any of the eight correlations. When the spacer design is neglected an accuracy of 10% can be considered satisfactory.

Table 1

Correlation	$Q_{DO,PRE}$ (MW)	E (%)
Barnett	1.67	−5.6
Becker	1.60	−9.6
Bezrukow	1.58	−10.7
Biasi	2.32	31.1
CISE 4	1.97	11.3
Condie & Bengston	1.52	−14.1
EPRI	1.61	−9.0
XN-1	1.74	−1.7

As previously mentioned, the total power hypothesis does not give any information about the axial location of the dryout. In the next paragraph, where the local hypothesis is employed, predictions of the dryout power as well as the axial dryout location will be presented.

6.2. Local hypothesis

The predictions with the local hypothesis are shown in figures 9–16. A summary of the predicted dryout powers and dryout locations is given in table 2. In the Oskarshamn 2 sub-bundle the power was, as previously mentioned, estimated at 1.77 MW, and dryout occurred on the corner pin facing the corner sub-channel on a stretch starting at $z \sim 310$ cm and ending at $z = 339$ cm. Neglecting the effect of the spacers one may then assume the middle value of $z = 324$ cm to be a best estimate of the dryout position. Experience from loop experiments and evidence from the hot cell investigations, however, points to the upper end of the region, just below the topmost spacer, as the actual starting point of the dryout.

With regard to the dryout power excellent predictions within 1% were obtained with the Barnett, Becker and Bezrukow correlations. Also the Condie & Bengston, EPRI and XN-1 correlations yield very good results. However, the Barnett correlation predicts the dryout location to be too close

Table 2

Correlation	$Q_{DO,PRE}$ (MW)	z_DO (cm)	E (%)
Barnett	1.78	353.1	0.6
Becker	1.77	324.8	0.0
Bezrukow	1.75	309.3	−1.1
Biasi	2.55	324.8	44.1
Condi & Bengston	1.68	309.3	−5.1
CISE 4	2.12	340.3	19.8
EPRI	1.73	341.6	−2.3
XN-1	1.90	324.8	7.3

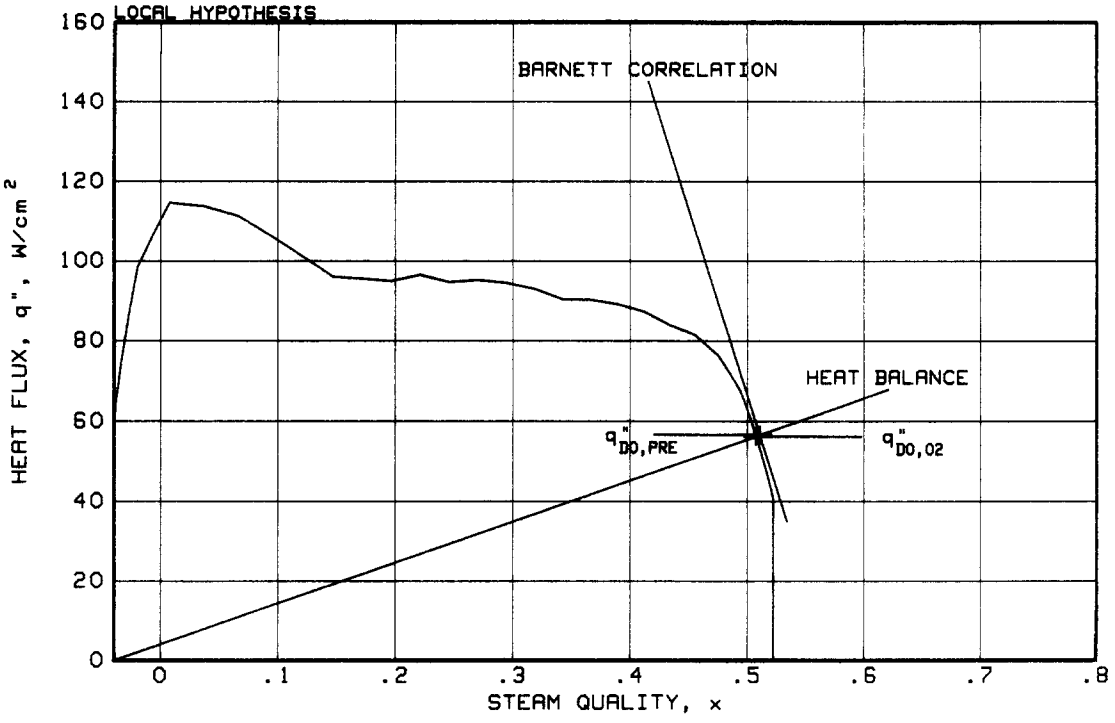

Figure 9. Comparison between measured and predicted dryout conditions. Barnett correlation.

to the end of the fuel bundle. The Becker and XN-1 correlations predict the dryout location to be the centre of the observed zone, the Bezrukow and Condie & Bengston correlations predict dryout at the lower end of the zone, while the EPRI correlation predicts dryout a few cm above the dryout zone. Remembering that the effects of spacers are not included in the calculations the latter results may also be considered to be satisfactory.

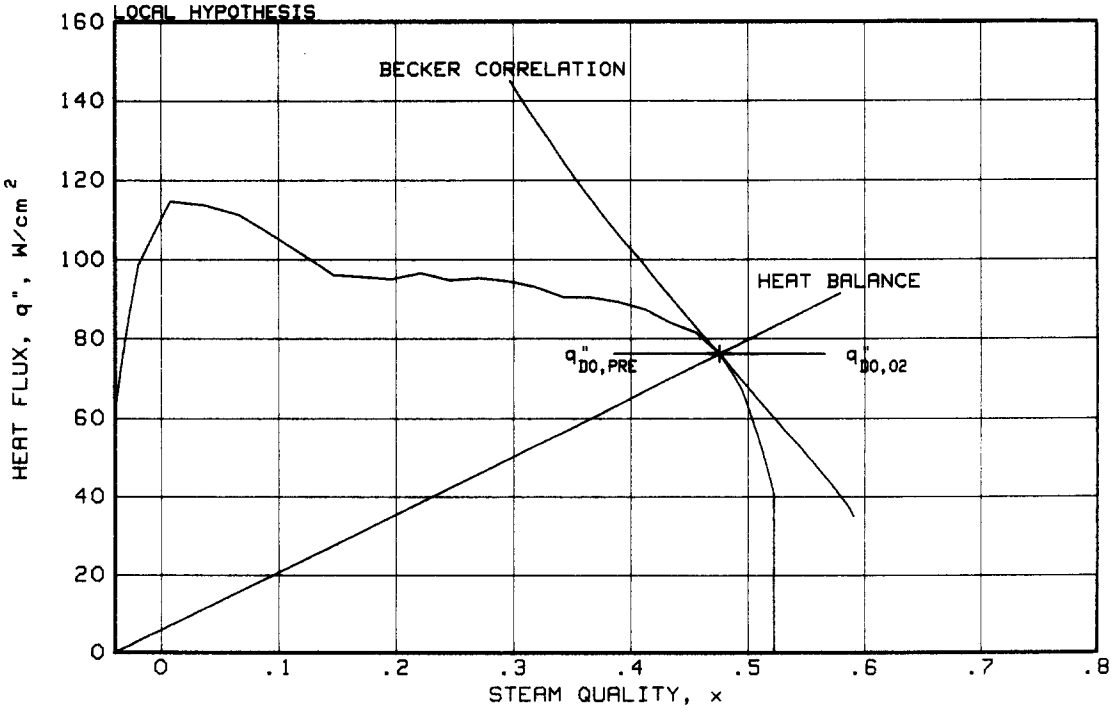

Figure 10. Comparison between measured and predicted dryout conditions. Becker correlation.

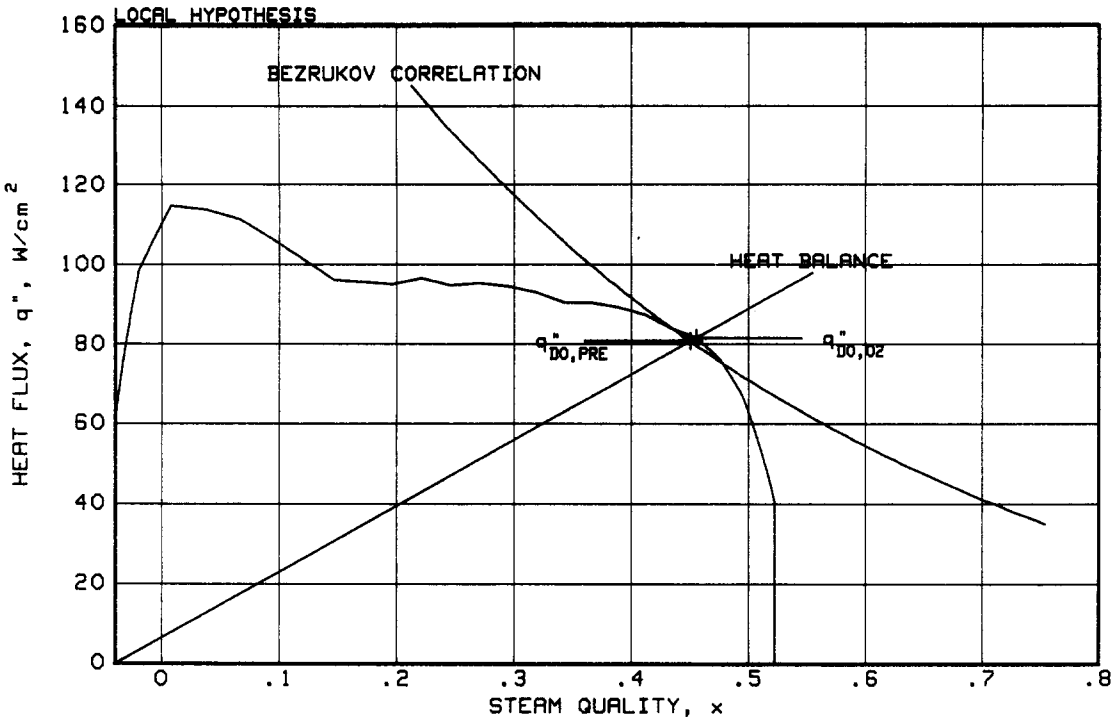

Figure 11. Comparison between measured and predicted dryout conditions. Bezrukov correlation.

The high dryout power obtained with the Biasi correlation was expected because this correlation is a round tube correlation and, thus, neglects the effects of the unheated walls of the rod bundle. As previously mentioned, the reason for including this correlation in the present analysis was the fact that the correlation has been used in the RELAP and TRAC computer programs.

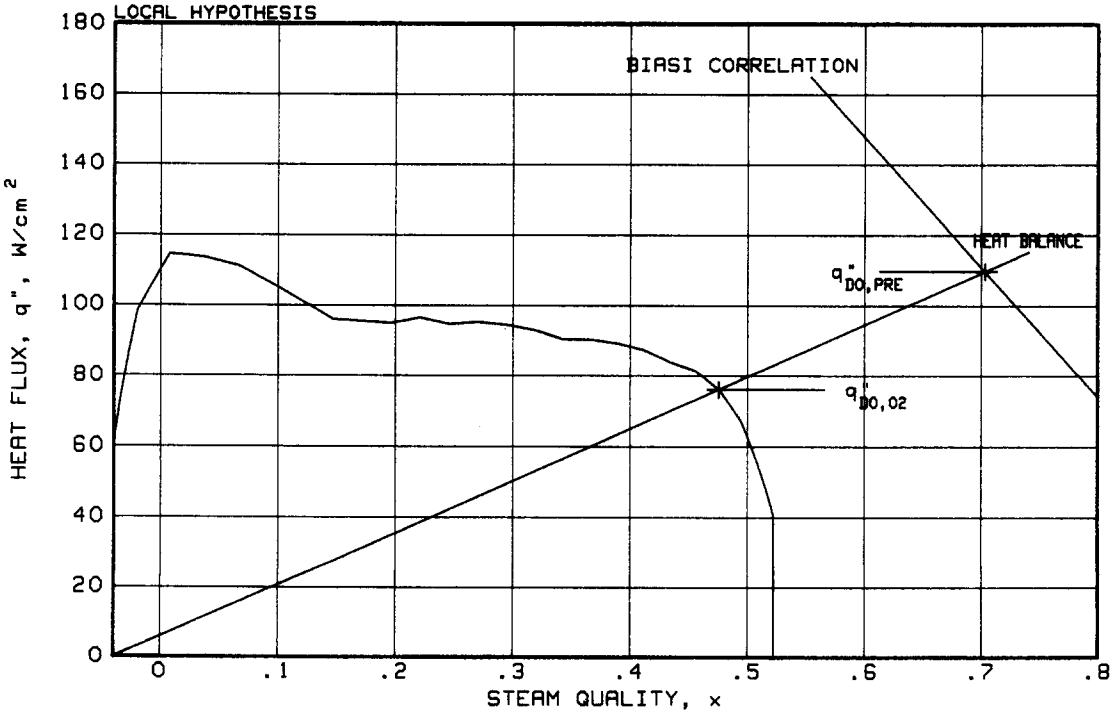

Figure 12. Comparison between measured and predicted dryout conditions. Biasi correlation.

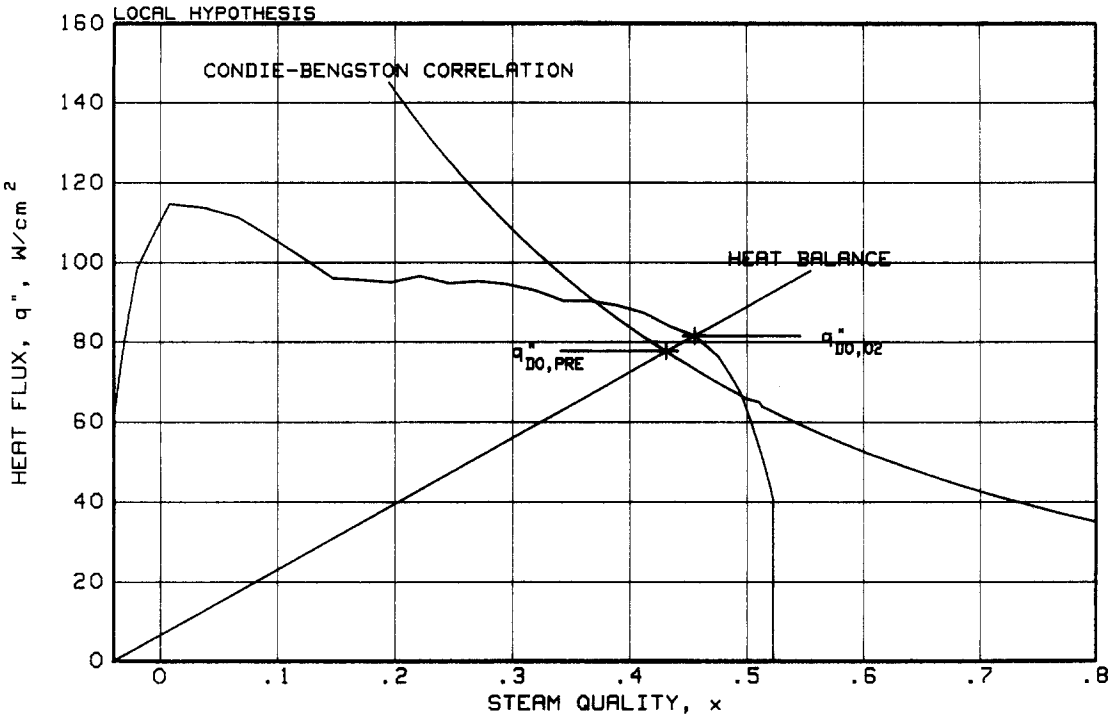

Figure 13. Comparison between measured and predicted dryout conditions. Condie & Bengston correlation.

It should also be recognized that the circumferential heat flux variation was neglected in the dryout analysis. In the corner sub-channel, where dryout occurred, the heat flux was up to 10% higher in comparison with the average value for the corner rod. This may seem to introduce an important uncertainty in the predicted dryout conditions. However, the experimental results by

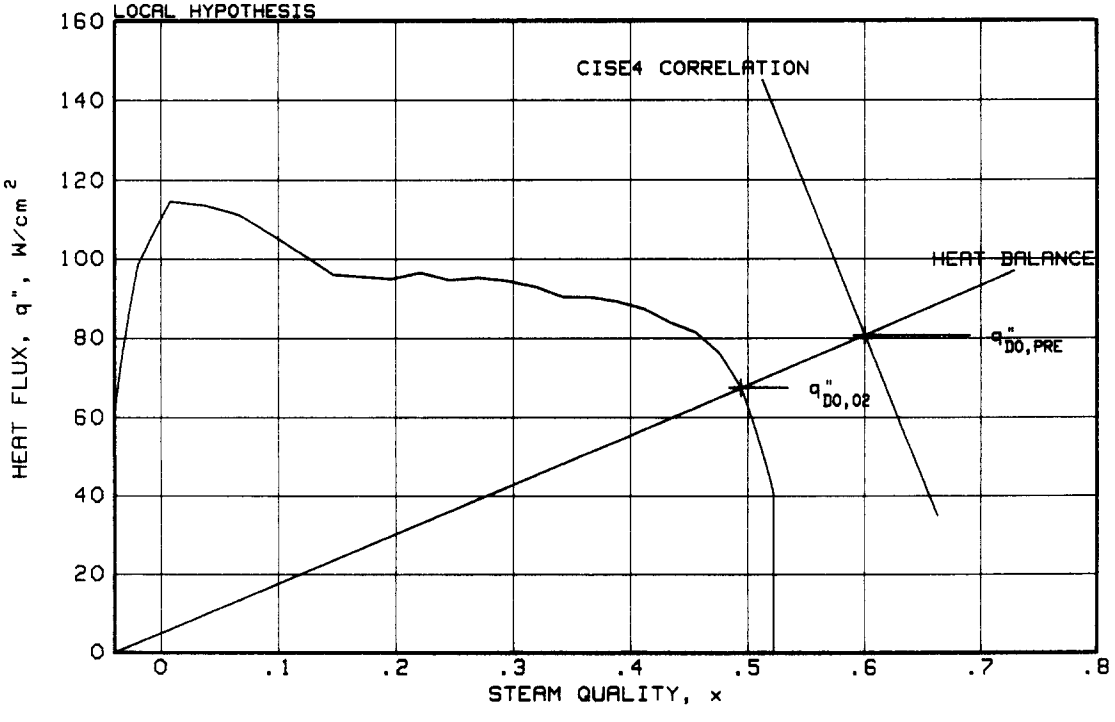

Figure 14. Comparison between measured and predicted dryout conditions. CISE 4 correlation.

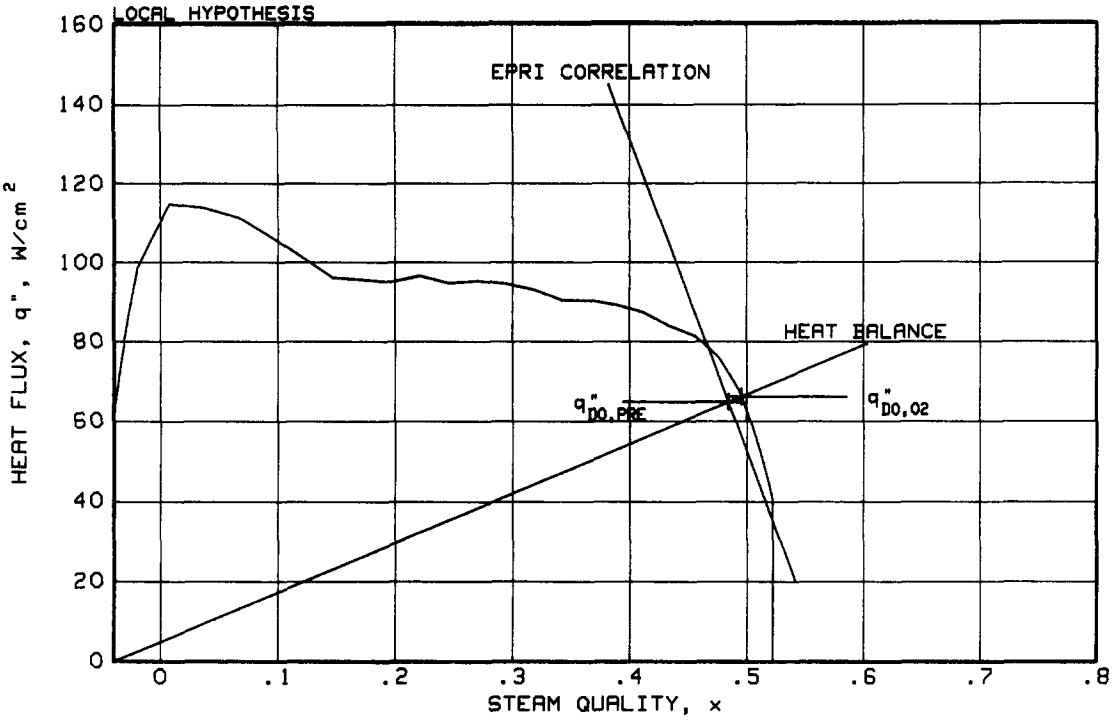

Figure 15. Comparison between measured and predicted dryout conditions. EPRI correlation.

Becker *et al.* (1988) for dryout in tubes with one-sided heating indicated a tangential flow of water in the liquid film on the tube wall, thus compensating for the circumferential heat flux distribution and yielding dryout powers very close to results obtained with uniformly heated tubes with the same length and diameter. The error introduced by neglecting the circumferential heat flux distribution is estimated at a few percent.

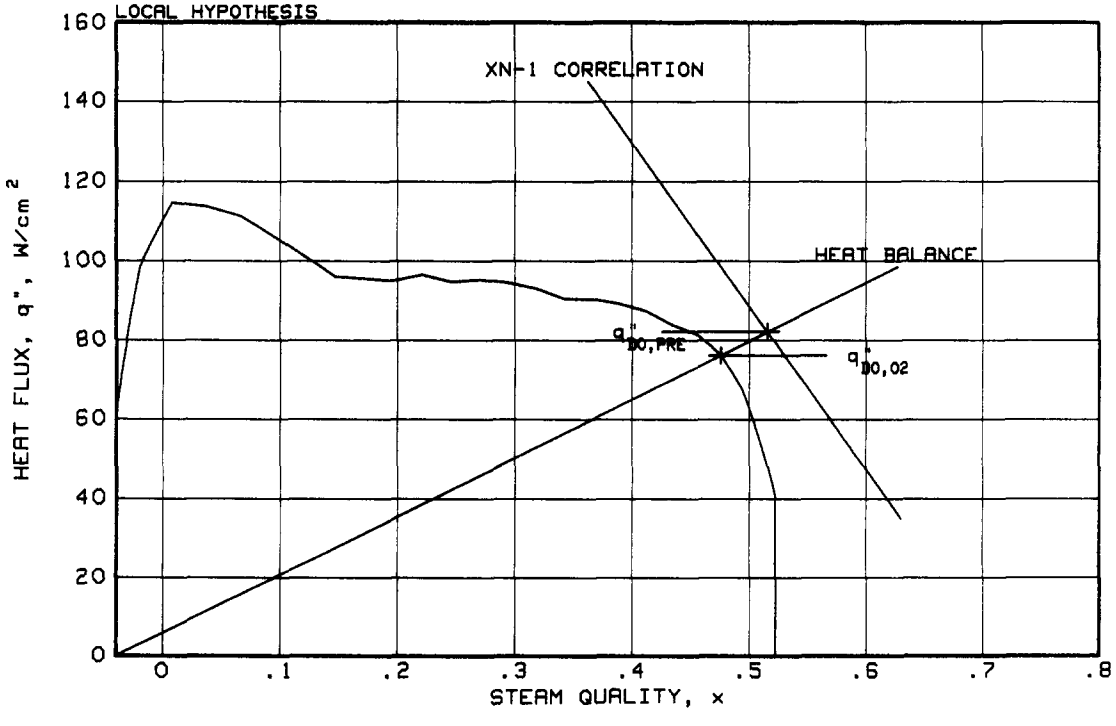

Figure 16. Comparison between measured and predicted dryout conditions. XN-1 correlation.

Reverting to table 2 one recognizes that six correlations predict the Oskarshamn 2 dryout power with errors between -5.1 and $+7.3\%$. Four of the correlations yield the axial dryout position within the damaged zone. These results confirm that the Oskarshamn 2 dryout incident was not caused by any mistakes in the design of the SVEA fuel or in the choice of the dryout margin. The failures are explained by the large channel bow, which develops when the channels are re-used. For future operation the present dryout margins need not to be changed. However, the effects of the channel bow must be included in the core supervision calculations.

It should also be recognized that the input to the present dryout analysis was obtained from physics and thermo-hydraulic calculations, where the POLCA, PHOENIX, CASMO and CONDOR computer programs were employed. There are of course uncertainties in this analysis, particularly with regard to the assumption of an axial mean channel bow of about 60% of the measured mid-channel bow at the end of the cycle. Work is still in progress to improve the knowledge of the actual conditions as far as possible.

The actual power for onset of dryout has been somewhat exceeded during the incident. The fact that the damage was obtained only in the zone below the topmost spacer indicates that the limit was only marginally exceeded. Experience from loop tests suggests that damage would otherwise also have been obtained just below the next spacer in the upstream direction at $z \sim 280$ cm. Reverting to figure 4 one observes that two of the rods, which are neighbours to the corner rod, had local peaking factors of 1.36, while the value for the corner rod was 1.38. This difference, which is $< 1.5\%$ suggests that also these rods should have been close to dryout. However, none of them were damaged.

It is therefore concluded that the dryout conditions for the corner rods are accurately defined. With the reservation for some remaining uncertainties in the initial analysis the Oskarshamn 2 incident therefore represents a very good base for assessments of dryout correlations.

6.3. Correlation used in core supervision

The core supervision of the SVEA assemblies in Oskarshamn 2 relies on the commercial AA-74A correlation, which is based on extensive full-scale testing with spacers of the same type as in the reactor fuel. It includes a simplified sub-channel model that accounts for the local power distribution within the sub-bundles, and a routine that handles the power and flow mis-match between the sub-bundles. For the present case it gave a dryout power, which was 7% too high. Considering the uncertainties involved in this comparison of a quite extreme situation, as discussed above, that discrepancy may not be too surprising. However, because of the importance for the core supervision there is a continued effort to identify possible errors in all steps involved, and thus to be able to further improve the overall accuracy of the in-core dryout evaluation.

7. POST-DRYOUT TEMPERATURES

Metallurgical investigations of the fuel rod materials in the dryout zone were carried out by Jonsson (1989). These studies revealed that the temperature of the canning had reached ~ 1000°C. This temperature was much higher than expected, and comparisons with the post-dryout heat transfer correlations by Groeneveld (1975) and Groeneveld & Delorme (1976) were therefore carried out. The following wall temperatures were obtained:

Groeneveld (1975)	$T_w = 800$°C
Groeneveld & Delorme (1976)	$T_w = 830$°C.

The latter correlation takes into account the thermodynamic non-equilibrium in the post-dryout flow region and is therefore considered to be the most accurate.

In the calculations the local mass velocity and the local steam quality in the corner sub-channel were used. These values were obtained by means of the COBRA computer program. With regard to the surface heat flux of that part of the fuel rod, which faced the corner sub-channel, the circumferential heat flux variation was included by multiplying the average rod heat flux by a factor of 1.10.

The Groeneveld & Delorme (1976) prediction of the wall temperatures seems to be ~ 170°C low in a direct comparison with the results of the metallurgical investigations. However, taking into

account that the temperature of the remaining metal in the dryout position has been successively increased due to oxide formation and correspondingly reduced heat conduction, both predictions seem to give very reasonable results for the actual surface temperature. Some uncertainty is also due to the prediction of the mass velocity in the corner sub-channel with the COBRA program.

8. CONCLUSIONS

On the basis of the present work the following conclusions were obtained:

1. Several rod bundle dryout correlations, which are available in the open literature, predict accurately the dryout conditions for the Oskarshamn 2 dryout incident.
2. The effects of irradiation on channel bow should be recognized as a serious core supervision problem, and the re-use of channels should therefore be avoided.
3. The effects of channel bow should be incorporated in the calculations of the power distributions in the fuel assemblies. If this is considered it is not necessary to change the dryout margin.
4. The dryout in the Oskarshamn 2 reactor was not caused by any faults in the design or manufacture of the fuel.

Acknowledgement—The present research was sponsored by OKG AKTIEBOLAG. Their financial support is gratefully acknowledged.

REFERENCES

BARNETT, P. G. 1966 A correlation of burnout data for uniformly heated annuli and its use for predicting burnout in uniformly heated rod bundles. Report AEEW-R463.

BECKER, K. M. 1967 A burnout correlation for flow of boiling water in vertical rod bundles. Report. AE-276.

BECKER, K. M., HERNBORG, G., BERGMAN, K. & LANGE, S. 1969 Measurements of burnout conditions in vertical round tubes with non-uniform axial heat flux. Report AE-RL-1153.

BECKER, K. M., ENERHOLM, A., SARDH, L., KÖHLER, W., KASTNER, W. & KRÄTZER, W. 1988 Heat transfer in an evaporator tube with circumferentially non-uniform heating. *Int. J. Multiphase Flow* **14,** 575–586.

BERTOLETTI, S., GASPARI, G. P., LOMBARDI, C., PETERLONGO, G., SILVESTRI, M. & TACCONI, F. A. 1965 Heat transfer crisis with steam–water mixtures. *Energia Nucl., Milano* **12.**

BEZRUKOW, Y. A., ASTAKHOV, V. I., BRANTOV, V. G., ABRAMOV, V. I., TETSOV, I. I., LOGVINOV, S. A. & RASSOKHIN, N. G. 1976 Experimental investigation and statistical analysis of data on burnout in rod bundles for water-moderated water-cooled reactors. *Teploenergetika* **23,** 67–70.

BIASI, L., CLERICI, G. C., GARRIBBA, S., SALA, R. & TOZZI, A. 1967 Studies on burnout, Part 3. A new correlation for round ducts and uniform heating and its comparison with world data. *Energia Nucl., Milano* **14.**

CONDIE, K. G. & BENGSTON, S. J. 1978 Development of the MOD7 CHF correlation. Report PN-181-76, EG & G, Idaho.

EDENIUS, M. & AHLIN, Å. 1988 CASM0-3: New features, benchmarking and advanced applications. *Nucl. Sci. Engng* **100,** 342–351.

GASPARI, G. P., HASSID, S. & LUCCHINI, F. 1974 A rod centered subchannel analysis with turbulent enthalaphy mixing for critical heat flux predictions in rod clusters cooled by boiling water. Presented at the *5th Int. Heat Transfer Conf.*, Tokyo.

GROENEVELD, D. C. 1975 Post-dryout heat transfer: physical mechanisms and a survey of prediction methods. *Nucl. Engng Des.* **32,** 283–294.

GROENEVELD, D. C. & DELORME, G. G. J. 1976 Prediction of thermal non-equilibrium in the post-dryout regime. *Nucl. Engng Des.* **36,** 17–26.

JONSSON, T. 1989 Investigation of failed fuel from Oskarshamn 2 1988. Final Report SE NF(P)-89/40 (in Swedish).

LEE, D. H. & OBERTELLI, J. D. 1963 An experimental investigation of forced convection burnout in high pressure water—II. Preliminary results for round tubes with non-uniform axial heat flux distribution. Report AEEW-R309.

LILES, D. R. & MAHASSI, J. H. 1986 TRAC-PF1/MOD1: an advanced best-estimate computer program for pressurized water reactor thermal-hydraulic analysis. Report NUREG/CR-3858/LA-10157-MS.

LINDAHL, S. Ö. 1983 CORE MASTER—the ASEA ATOM core analysis system. Presented at the *ANS Top. Mtg on Reactor Operating Experience*, Scottsdale, Ariz.

LITTLE, R. B. 1970. Dryout tests on an internally heated annulus with variation of axial heat flux distribution. Report AEEW-R578.

OLSSON, S. 1983 The PHOENIX–POLCA calculation system. Presented at *Status of Static Reactor Calculations in Nordic Countries*, Gothenburg.

RANSOM, V. H., WAGNER, R. J., TRAPP, J. A., FEINAUER, L. R., MILLER, C. S. & JOHNSEN, G. W. 1985 RELAP5/MOD2 code manual, Vols 1 & 2. Report NUREG/CR-4312.

REDDY, D. G. & FIGHETTI, C. F. 1983 Parametric study of CHF data, Vol 2. Report EPRI NP-2609.

STAMM'LER, R. J. J. & VEENHUIZEN, H. P. 1987 PHOENIX: outstanding features; verification in critical experiments and against gamms detector measurements in Ringhals 1. Presented at *AND/END Int. Top. Mtg on Advances in Reactor Physics, Mathematics and Computation*, Paris.

STEVES, L. H., SUTEY, M. A. & FITZSIMMONS, D. E. 1972 XN-1 critical heat flux correlation for boiling water reactor fuel. Report JN-72-18.

TONG, L. S. 1965 Influence of axially non-uniform heat flux on DNB. Report WCAP-2767.